Geomechanics and Engineering, *Vol. 29, No. 2 (2022) 171-182*
https://doi.org/10.12989/gae.2022.29.2.171

Evaluation of long term shaft resistance of the reused driven pile in clay

Jifei Cui[a], Pingping Rao[b], Jian Wu[c] and Zhenkun Yang*

Department of Civil Engineering, University of Shanghai for Science and Technology, Shanghai 200093, China

(Received October 22, 2021, Revised February 19, 2022, Accepted March 8, 2022)

Abstract. Reusing the used pile has not yet been implemented due to the unpredictability of the bearing capacity evolution. This paper presents an analytic approach to estimate the sides shear setup after the dissipation of pore pressure. Long-term evolution of adjacent soil is simulated by viscoelastic-plastic constitutive model. Then, an innovative concept of quasi-overconsolidation is proposed to estimate the strength changes of surrounding soil. Total stress method (α method) is employed to evaluate the long term bearing capacity. Measured data of test piles in Louisiana and semi-logarithmic time function are cited to validate the effectiveness of the presented method. Comparisons illustrate that the presented approach gives a reasonably prediction of the side shear setup. Both the presented method and experiment show the shaft resistance increase by 30%-50%, and this highlight the potential benefit of piles reutilization.

Keywords: driven pile; long term; quasi-overconsolidation ; reuse; side shear setup

1. Introduction

Construction industry was responsible for a large proportion of worldwide resources and energy consumption and emitted a lot of greenhouse gases (Chou and Yeh 2015).

In China, about 300 million meters of concrete pipe piles were consumed in 2017. Raw materials of concrete piles, such as aggregate, sand and steel, are unrenewable resources. Besides, buildings constructed in early years, such as coastal high-piled wharf and factories, are out of date and unable to meet the demands of rapid economy growth in China. Most of them need to be demolished and rebuilt. Superstructure concrete of the demolished buildings can be reused via recycled aggregate concrete (Wijayasundara *et al*. 2018, Xiao *et al*. 2018a, b), but plenty of piles are left in the strata (Ko *et al*. 2018). At present, two approaches to deal with the left piles are removal and avoidance, but both of them will bring about enormous material and energy waste. Moreover, avoidance will place restrictions on the layout of new piles and remove will disturb the site soil and weaken the shaft resistance of the newly driven pile. Reusing of these used piles in situ to bearing load together with newly driven piles is a sustainable approach. But the wider application of used piles is still restricted because of the difficulties in evaluating their bearing capacity. Evaluating the bearing capacity of used pile is the premise of reuse and joint bearing design of used and new piles.

Both laboratory and field tests show that soil exhibits time-dependent behavior, and the result is that soil gains additional strength with time. Therefore, the pile bearing capacity increases after EOD (end of driving), which is called "setup". Used concrete driven piles of a glass factory were tested before they were reused as foundations for new residential buildings by the authors. Comparison between the static load test of the used piles and newly driven piles illustrates a marked increase of both the bearing capacity and stiffness. Bullock *et al*. (2015a, b) conducted a test pile program and measured the shaft resistance for up to 4.7 years and observed that bearing capacity increase by 30% - 50%. Thompson *et al*. (2009) reported an increase in side shear between 1.8 and 3 times of the side shear at the end of driving (EOD) in soft stratum along the Mississippi Gulf Coast. Doherty and Gavin (2013) launched a series of field tests about the time effect of driven pile in soft stratum which was lasted for 10 years. The results show that the bearing capacity increased by 30% during this period. Skov and Denver (1988) put forward a logarithm relation between elapse time and bearing capacity. Many other researchers have developed similar empirical approaches (Augustensen *et al*. 2005, Huang 1988, Yang and Liang, 2006, Chen and Zhang 2022). However, despite the proposed empirical formulas, the explanation of the underlying mechanism and the analytic approach are still not available.

The setup mechanism is generally believed to be two aspects (Augustensen *et al*. 2005): (i) Short-term effects. Dissipation of pore pressure is the main reason, while aging (change in strength and stiffness due to the change in soil skeleton and stress regime with time) has also played a certain role (Xu *et al*. 2020, Li and Chang 2022); (ii) Long-term effects. Aging is the only reason in this stage (Chong *et al*. 2019, Zou *et al*. 2019). Many researchers have studied

*Corresponding author, Doctoral Candidate
E-mail: yang@lih.rwth-aachen.de
[a]Lecturer
E-mail: cuijifei@usst.edu.cn
[b]Professor
E-mail: raopingping@usst.edu.cn
[c]M.Sc. Student
E-mail: wujian6104@163.com

ISSN: 2005-307X (Print), 2092-6219 (Online)

the mechanism of excess pore pressure dissipation regarding short-term effects with the radial consolidation theory, and the analytical methods have been established (Basu *et al*. 1985, Kou *et al*. 2016, Kou *et al*. 2017, Li *et al*. 2017a, b, Cui *et al*. 2022). However, the aging effect causing long-term setup are complicated and not yet fully understood. Most of the current studies are based on experimental observations or empirical formulas. The aging effect has not been taken into account in theoretical analysis. Axelsson (1998, 2002) put forward that the gain in soil strength due to periods of creep volume change was the plausible reason for aging mechanism controlling long term setup for piles. Bullock *et al*. (2005b) found that pile got additional shaft resistance after the completion of dissipation of pore water pressure. Meanwhile, test results also showed the effective horizontal stress remain unchanged during this process, which means that the effective friction angle increases and indicates an evolution of the internal structures in adjacent soil. Bowman and Soga (2003) qualitatively analyzed the mechanism of pile setup based on restrained dilation theory and aging of surrounding soil. Cui *et al*. (2019) studied the evolution of the load transfer characteristic, which is applied to evaluate the load settlement characteristic of the old piles. Previous studies show that the side shear setup has much to do with aging effect, but there is no practical way of theoretical analysis. So it would be constructive and meaningful to quantify the aging effect on side shear setup of a driven pile.

This paper put forward a theoretical method to predict the long-term sides shear setup of used driven piles in clay. Quantifying the soil strength variation and applying it to determine the shaft resistance are two key steps to analyze the bearing capacity evolution of used piles. The evolution of surrounding soil behavior under normal loading state with time is simulated by the nonstationary flow surface (NSFS) elasto-viscoplastic constitutive model. Total stress method (α method) is adopted to determine the side resistance based on the concept of quasi-overconsolidation. Loading conditions, pile characteristics (diameter and length), and soil properties (especially the creep properties) effecting the time-dependent side resistance are reasonably considered in the proposed approach. Results of the test piles in Louisiana are cited here to validate the proposed method. Side shear setup factors are also investigated.

2. Stress state variation of the surrounding soil

Evolution of soil behaviors is closely related to the stress state during the elapsed time. For displacement piles, stress change of surrounding soil mainly occurs in two stages, pile penetration and loading. The adjacent soil is pressed primarily outward in the process of pile installation, as shown in Fig. 1 (Zhang *et al*. 2020, Chen and Mo 2022, Li *et al*. 2021, Yang *et al*. 2021, Chen *et al*. 2021a, b, Mo and Yu 2017, 2018, Zhou *et al*. 2018). Li *et al*. (2016) gave the effective stresses, σ', and the excess pore pressure, u_{e0}, at the critical region after pile penetration based on the K_0-consolidated anisotropic modified Cam-clay (K0-AMCC) model as follows

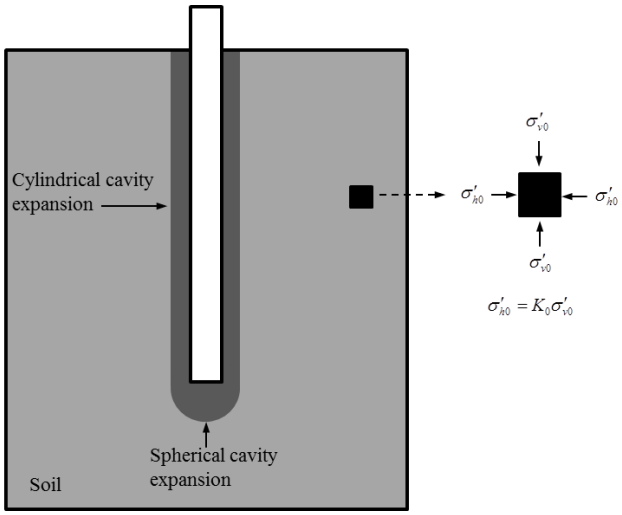

Fig. 1 Cavity expansion model for pile driving in clay

$$\begin{cases} \sigma'_{zf} = \dfrac{3}{2K_0+1}p'_f \\ \sigma'_{rf} = \dfrac{3K_0}{2K_0+1}p'_f + \dfrac{\beta}{2}p'_f \\ \sigma'_{\theta f} = \dfrac{3K_0}{2K_0+1}p'_f - \dfrac{\beta}{2}p'_f \end{cases} \quad (1)$$

$$u_{e0} = p'_0\left(\frac{3K_0}{1+2K_0} + \frac{\eta^*_p}{\sqrt{3}}\right) + p'_f\left(\beta\ln\frac{r_p}{r} - \frac{\beta}{2} \pm \frac{\sqrt{4M^2-3\beta^2}}{6} - 1\right) \quad (2)$$

where σ'_{zf}, σ'_{rf}, $\sigma'_{\theta f}$ are the principal stress components of σ', K_0 is the earth pressure coefficient, $p'_f = p'_0(OCR/2)^{\Lambda}$ and $q_f = Mp'_0(OCR/2)^{\Lambda}$ are the mean effective stress and the deviator stress in the surrounding plastic region, p'_0 is the in situ initial mean stress, OCR is the overconsolidation ratio, Λ is the plastic volumetric strain ratio, M is the stress ratio. The plus sign is used when $K_0 \le 1$; otherwise, the minus sign is used; η^*_p is the relative stress ratio; and r_p is the radius of the plastic region. β is determined by Eq. (3)

$$\beta = 2\sqrt{3[M^2(2K_0+1)^2 - 9(1-K_0)^2]}/[3(2K_0+1)] \quad (3)$$

The effective stress increase from σ' with time soon after the pile penetration was completed due to consolidation. Previous studies showed that pore water pressure entirely dissipates in short time, which mainly affects the short term side shear setup (Basu *et al*. 2014, Bullock *et al*. 2005b, Li *et al*. 2017a). Therefore, a hypothesis can be presented here that the pore pressure is completely dissipated immediately after pile installation.

This means the consolidation process is not involved here, while the effective stress increase induced by pore pressure dissipation is considered. The bearing capacity evolution within the short term was not accurately illustrated in this paper. But for the long term time dependent bearing capacity evolution, the method proposed in this paper has

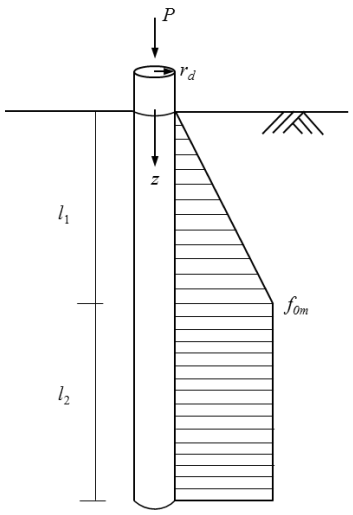

Fig. 2 Shaft resistance distribution

enough accuracy. The final effective stress, $\sigma_{t_0}^{'}$, can be determined as follow

$$\boldsymbol{\sigma}_{t_0}^{'} = \boldsymbol{\sigma}' + \xi u_{e0} \tag{4}$$

where ξ is transfer parameter, $\xi=(1+\nu')/3(1-\nu')$, ν' is Poisson's ratio.

The surrounding soil provides shaft resistance to resist the working load. Field tests indicated that the shaft resistance is first fully activated at the upper part of pile under the working load (Kou *et al*. 2017, Potts and Martins 1982). Based on the measured shaft resistance distribution of piles, the simplified bilinear patterns of the shaft resistance are suggested, as shown in Fig. 2. The working load *P* is borne by side friction resistance and the equilibrium relationship between the working load *P* and the shaft resistance can be expressed as follows

$$P = 2\pi r_d (\frac{1}{2} l_1 f_{0m} + l_2 f_{0m}) \tag{5}$$

where l_1 , l_2 are the lengths of the upper and lower parts respectively; f_{0m} is the maximum shaft resistance.

Then f_{0m} can be determined by

$$f_{0m} = P / \pi r_d (l_1 + 2l_2) \tag{6}$$

Combined with Fig. 2, the shaft resistance can be given as follows

$$f_0 = \begin{cases} \dfrac{z}{l_1} f_{0m} & (z \le l_1) \\ f_{0m} & (z > l_1) \end{cases} \tag{7}$$

Due to the pile penetration and loading, the stress of soil adjacent to pile changed significant (Fig. 3). The stress state can be obtained as Eq. (8):

$$\boldsymbol{\sigma} = \boldsymbol{\sigma}_{t_0}' + \begin{bmatrix} 0 & f_0 & 0 \\ f_0 & 0 & 0 \\ 0 & 0 & 0 \end{bmatrix} \tag{8}$$

3. Evolution of the adjacent soil behaviors with time

Many researches aimed at predicting long-term behavior of soils through empirical, rheological, and general stress-strain-time theory (Augustesen *et al*. 2004, Liingaard *et al*. 2004, Yin *et al*. 2010, Karim and Gnanendram 2014).

Models based on general stress-strain-time theory can be divided into three categories (Sekiguchi 1984, 1985): (1) Models based on overstress theory (Perzyna, 163, 1966; Sivasithamparam *et al*. 2015). (2) NSFS models. The NSFS theory assumes the yield surface flows with time and satisfies the consistency requirement (Qiao *et al*. 2016, Sekiguchi 1997a, b, 1984). (3) Others (Borja and Kavazanjian 1985, Zhou *et al*., 2005).

The NSFS theory is employed here to simulate the aging behaviors of surrounding soil. According to the NSFS theory, viscoplastic strains take place while the soil is loading to the current yield surface. Then the yield surface expands outward while the stress remains unchanged (Qiao *et al*. 2016). The NSFS theory was distinguished from the classical elastoplasticity theory with the definition of the yield surface, which does not change with time in the classical theory. Based on the NSFS theory, accumulation of plastic volumetric strain will react on volumetric strain rate and the relationship between volumetric strain rate $\dot{\upsilon}(t)$ and volumetric strain $\upsilon(t)$ can be expressed as

$$\dot{\upsilon}(t) = \dot{\upsilon}_0 \exp\left[\frac{\bar{h} - \upsilon(t)}{\alpha}\right] \tag{9}$$

where $\dot{\upsilon}_0$ and α is model parameters, $\bar{h}$ is a scalar function with regard to $\bar{p}$ and $\bar{q}$ can be determined as

$$\bar{h} = \frac{\lambda}{1+e_0} \ln(\bar{p} / p_0) + D(\bar{q} / \bar{p} - q_0 / p_0) \tag{10}$$

where $\bar{p}$ is the mean normal stress, $\bar{q}$ is the generalized stress deviator, D is the parameter considering (negative) dilatancy effect (Shibata 1963). λ is the compression index.

The secondary compression index α was first applied to describe the aging effect of soil by Sekiguchi and Ohta. It can be determined by the coefficient of secondary compression C_α as

$$\alpha = 0.434 \frac{C_\alpha}{1+e_0} \tag{11}$$

Mesri and Godlewski (1977) pointed out that the secondary consolidation coefficient C_α is correlated with compression index C_c. $C_\alpha/C_c=\eta$ is a constant. For most inorganic clays, $\eta=0.04\pm0.01$; for highly plastic clay, $\eta=0.05\pm0.01$.

Compression index C_c can be obtained by laboratory test. Terzaghi and Peck (1968) suggest that C_c can also be determined as follow when the laboratory test is lacking.

$$C_c = 0.009(w_L - 10) \tag{12}$$

where w_L is the liquid limit.

$\dot{\upsilon}_0$ is the reference volumetric strain rate and was proposed by Sekiguchi (1977a, b). $\dot{\upsilon}_0$ can be determined by

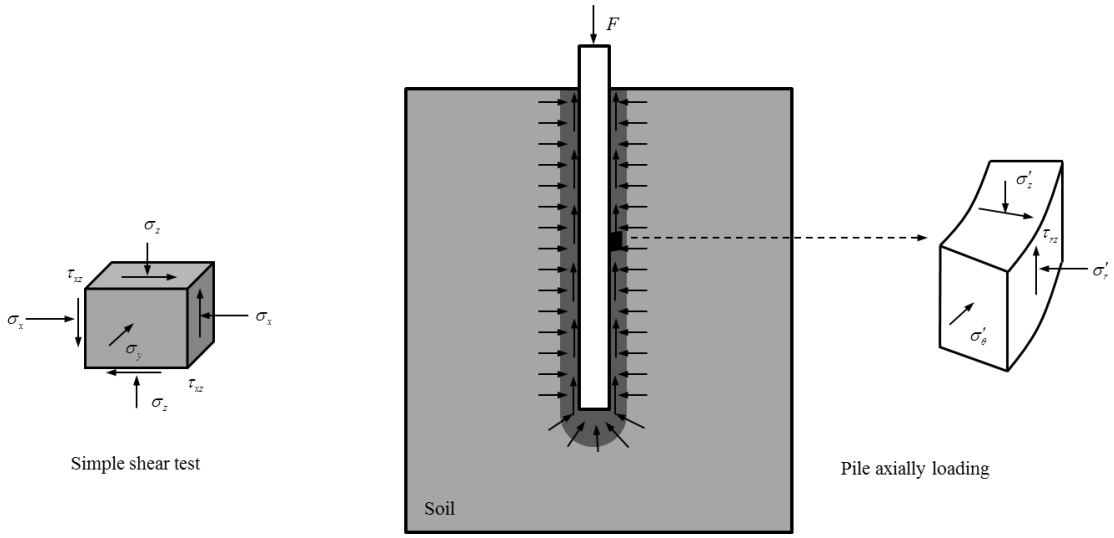

Fig. 3 Stress state of the surrounding soil and the soil sample in simple shear test

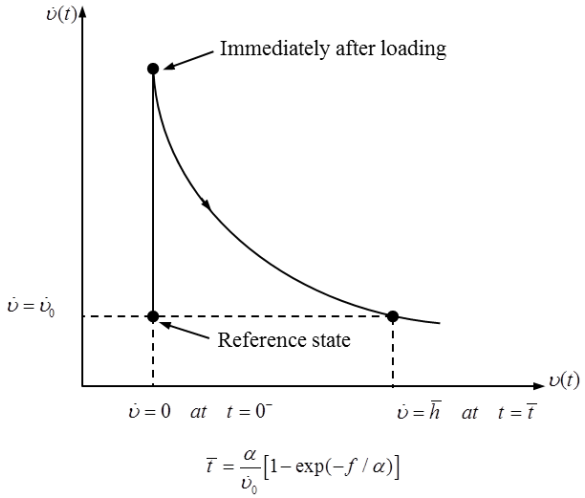

Fig. 4 Variation of volumetric creep rate with volumetric strain

$$\dot{\upsilon}_0 = \frac{\alpha}{t_c} \tag{13}$$

where t_c is the reference time.

D was first proposed by Shibata (1963). Shibata (1963) pointed out that the volume change during a σ_m'-const.-test is a proportional function of $(\sigma_1\text{-}\sigma_3)/\sigma_m'$ and the proportionality coefficient between them is defined as D.

The value of D is related to the soil moisture content to a great extent. Shibata (1963) also gave the D value of three soil samples with different moisture content by experiment. The D value of Fukuoka clay with moisture content between 71%-83% is 0.092. The D value of London clay with moisture content between 27%-35% is 0.077. The D value of Wead clay with moisture content between 18%-23% is 0.045. Hence, the value of D can be determined by the moisture content of the surrounding soil given in the test report and the range of D given by Shibata (1963) when the laboratory test is lacking.

Fig. 4 (Sekiguchi 1977a, b, 1984) shows the feature of the volumetric creep rate with volumetric strain. The volume strain accumulates gradually with time and the volume strain rate decreases in response. The volumetric strain can be obtained as the solution of following basic differential equation

$$\upsilon(t) = \frac{\kappa}{1+e_0}\ln(\bar{p}'/p_0') + \alpha \ln\left[1+\frac{\dot{\upsilon}_0 t}{\alpha}\exp(\bar{f}/\alpha)\right] \tag{14}$$

where

$$\bar{f} = \frac{\lambda-\kappa}{1+e_0}\ln(\bar{p}'/p_0') + D(\bar{q}/\bar{p}' - q_0/p_0') \tag{15}$$

where κ is the swelling index.

The first part in Eq. (14) represents the immediate elastic component of the volumetric strain. This means that the shear-induced volumetric strain (dilatancy) is assumed to be of a totally irreversible nature. The second part represents the viscoplastic (i.e., delayed, irreversible) component of volumetric strain and can be denoted as

$$\upsilon^p(t) = \alpha \ln\left[1+\frac{\dot{\upsilon}_0 t}{\alpha}\exp(\bar{f}/\alpha)\right] \tag{16}$$

The accumulation of volume strain with time leads to a reduction of the void ratio (e), which means that the soil has reached a more stable state. The relationship between volume strain and the reduction of the void ratio can be expressed as Eq. (17) according to the geometric equation.

$$\upsilon^p(t) = \frac{\Delta e(t)}{1+e_0} \tag{17}$$

Fig. 5 indicates that the surrounding soil will becomes more compact with time due to the aging effect. The amount of compression from A to A' in Fig. 5 can be determined by Eq. (17). The amount of compression from A to A' in Fig. 5 can also be reached by the path of normal over consolidation. Firstly, the soil was loading along the

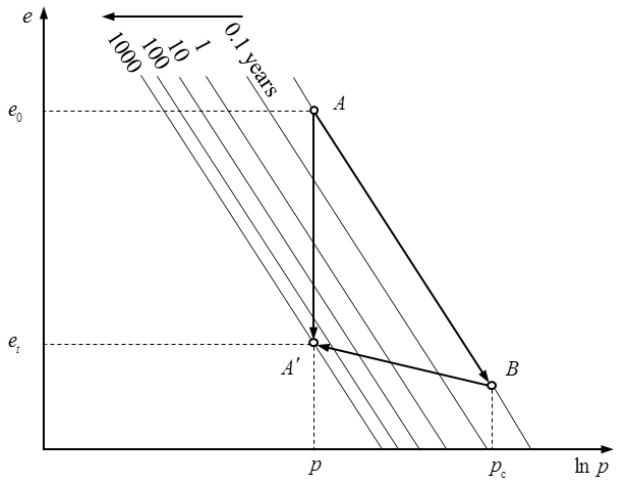

Fig. 5 Visualization of age dependency of soil

compression line to point *B*. Then the soil was unloading along the swelling line to point *A′*. These two different paths indicate that the aging effect brings about a steadier soil structure and a larger pre-consolidation pressure.

Clay that has just completed seepage consolidation is called normal compacted clay. Clay that has experienced aging (or delayed compaction) is called normally consolidated aged clay. In order to distinguish the over consolidation caused by unloading, the kind of overconsolidation related to the aging found in soil adjacent to the pile that has never experienced the usual cause of overconsolidation is referred to as quasi-overconsolidation (Q.O.C) or normal consolidation aged clay in this paper. Quasi-overconsolidation ratio (*QuOCR*) can be determined by

$$QuOCR(t) = \frac{p'_Q}{\overline{p}'}(t) = \exp\left(\frac{\Delta e(t)}{\lambda - \kappa}\right) \tag{18}$$

Then, the undrained shear strength $s_u(t)$ of the adjacent soil can be determined based on the MCC model as follows

$$s_u(t) = \frac{1}{2}\overline{p}' M \left(\frac{QuOCR(t)}{2}\right)^{\Lambda} \tag{19}$$

Eqs. (14)-(19) explicate the mechanism of side shear setup under a normal bearing state. Soil gains additional strength with time due to periods of aging volume change.

4. Evolution of the adjacent soil behaviors with time

The methods for calculating shaft resistance can be categorized as total stress (α) method, the effective stress (β) method, and other empirical methods. The total stress (α) method is commonly used to determine the ultimate side shear of driven pile. Therefore, the total stress (α) method is adopted in this paper to calculated the shaft resistance of the pile.

As shown in Fig. 3, the adjacent soil element has same stress state as the specimen of the simple shear test (Randolph and Wroth 1981). The maximum shear stress τ_{xz} can then be taken as the ultimate side shear f_s , which can be derived from the failure stress in a simple shear test as follows

$$f_s = \tau_{zx} = s_p \cos\phi' \tag{20}$$

where s_p is the shear strength of simple shear test. ϕ' is the effective internal friction angle.

Soil shows different shear properties in triaxial and simple shear tests. The soil strength determined by Eq. (19) is under triaxial state, which has to be converted to s_p. Matsuoka *et al*. (1977) put forward an approach to obtain s_p from s_u by a conversion coefficient. Then s_p can be determined by

$$s_p = \frac{3\sqrt{3}\sin\varphi_f}{2M\cos\psi_f\sqrt{2+\sin^2\varphi_f}} s_u \tag{21}$$

where φ_f and ψ_f can be determined by Eqs. (22) and (23) as follows

$$\sin\varphi_f = \frac{\sqrt{2}M}{\sqrt{9+3M}} \tag{22}$$

$$\psi_f = \frac{1}{3}\cos^{-1}\left\{-\left(\frac{3}{2+\sin^2\varphi_f}\right)^{3/2}\sin\varphi_f\cos 3\theta\right\} \tag{23}$$

5. Verification and discussion

5.1 Field test

To verify the proposed analytical approach, the side shear f_s obtained by the analytical approach is compared with the test results obtained by the Louisiana State University (Murad *et al*. 2016) in this section. Twelve prestressed concrete (PSC) piles were driven in five sites in Louisiana. Comprehensive laboratory and field tests were

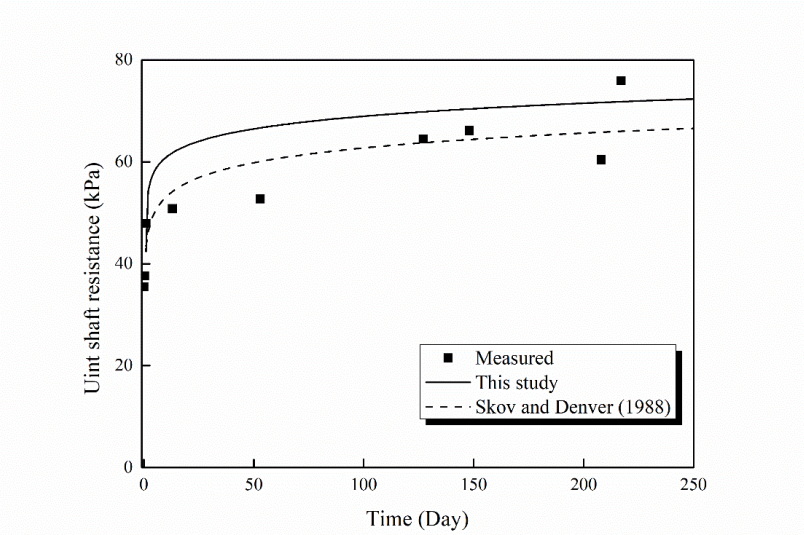

Fig. 6 Comparisons between predicted, measured and semi-logarithmic time function values at the depth of 14.3 m of TP1

carried out at each site to obtain the detailed physical and mechanical parameters of soil. The static load tests were conducted at different times after end of driving (EOD) to measure the evolution of the bearing capacity of the driven piles and to quantify the sides shear setup. Vibrating wire strain gages were instrumented on the test piles to obtain the distribution of load transfer along the length of the piles. The shear forces were calculated from the difference in axial force between two adjacent strain gauges. Based on investigation up to more than 200 days, the long-term side shear setup was studied. Two test piles (TP-1 and TP-3) in Bayou Lacassine Site are cited here to validate the effectiveness of the presented method. The sides of the pile were 760 mm in width. The total length of TP-1 and TP-3 were 22.86 m, and the test piles TP-1 and TP-3 were installed 20.42 m below the ground surface. The unit side shear for each soil layers of TP-1 and TP3 at each test time after the end of driving (1, 13, 53, 127, 148, 208, 217 days for TP-1 and 1, 15, 29, 93, 129, 175, 185 days for TP-3) was presented in the report (Abu-Farsakh *et al*. 2016).

5.2 Semi-logarithmic time function

Skov and Denver (1988) proposed a semi-logarithmic time function to simulate the capacity evolution with time by the following form

$$Q = Q_0 \left\{ 1 + \Delta_{10} \log_{10} \left\{ \frac{t}{t_0} \right\} \right\} \tag{24}$$

where Q_0 is the capacity at t_0 when pore water pressure has dissipated, and Δ_{10} is the empirical coefficient.

However, Q_0 involves both base resistance and side resistance, while the theoretical method proposed in this paper can only evaluate the evolution of the side resistance. Therefore, the semi-logarithmic time function presented in this section concerns the pile side resistance only. The semi-logarithmic time function is modified as follows

Table 1 Properties of the surrounding soil

Soil property	TP-1(14.3 m)	TP-3(8.84 m)
Compression indice [λ]	0.15	0.12
Swelling indice [κ]	0.05	0.05
Moisture content[ω]	24.65%	26%
Liquid limit [w_L]	50	44
Secondary compression index [α]	0.0038	0.0033
Coefficient of (negative) dilatancy [D]	0.065	0.07
Reference volumetric strain rate [$\dot{v}_0$(min^{-1})]	2.67×10-6	2.27×10-6

$$f_s(t) = f_{s0} \left\{ 1 + \Delta'_{10} \log_{10} \left\{ \frac{t}{t_0} \right\} \right\} \tag{25}$$

where Δ'_{10} is side (segment) shear setup factor, $f_s(t)$ is the side resistance at elapsed time t after pile penetration, f_{s0} is the side resistance at t_0 when pore water pressure has dissipated.

5.3 Comparison with the analytical approach, the test result and the semi-logarithmic time function

Comparisons of the test result and semi-logarithmic time function with the presented analytical approach on unit side shear are shown in Figs. 6 and 7. The test result in Figs. 6 and 7 are unit side shear of TP-1 at depths of 14.3 m and TP-3 at depths of 8.84 m, respectively. The soil parameters (shown in Table 1) are determined by the aforementioned procedure and the laboratory and in-situ soil testing given in the report (Abu-Farsakh *et al*. 2016).

Fig. 6 shows a good agreement of the predicted results with the test values as well as the semi-logarithmic time function. This confirms the validity of the method proposed in this paper. It is worth noting in Fig. 6 that the sides shear

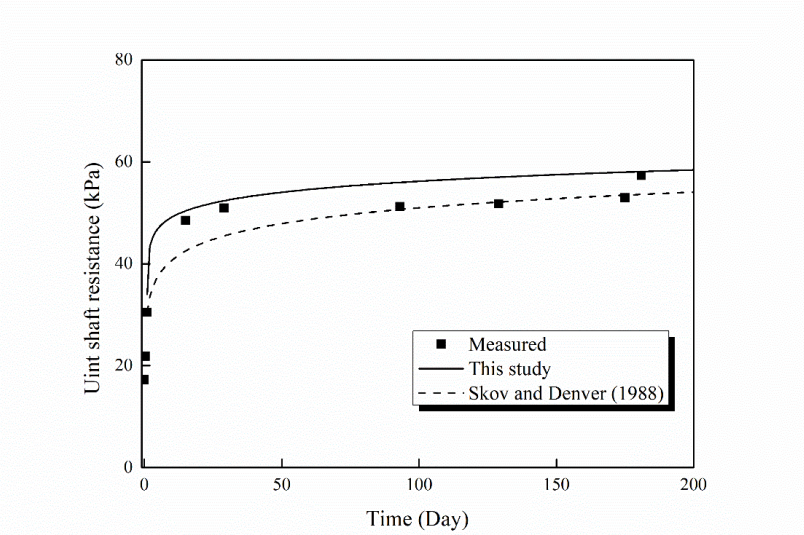

Fig. 7 Comparisons between predicted, measured and semi-logarithmic time function values at the depth of 8.84 m of TP3

increases with a relatively higher rate during the first 50 days after pile penetration. Thereafter, the increasing velocity decrease with time due to the accumulation of the volumetric strain, $\upsilon(t)$. The unit shaft resistance at depths of 8.84 m of TP-3 is presented in Fig. 7, which also shows reasonable accordance among the test results, the semi-logarithmic time function and the presented analytical method.

Fig. 6 and 7 also illustrate that the proposed analytical results are higher than the measured values at early stage. It is because of the hypothesis of the proposed approach that the excess pore pressure induced by pile penetration has been completely dissipated before aging of the soil. The contribution of the consolidation has been considered initially, although the process of the excess pore pressure dissipation is beyond the scope of the approach in this paper. So the proposed approach may overestimate the shaft resistance at the initial stage. Nevertheless, the pore pressure dissipates at a quicker rate than aging. Hence the proposed approach can reasonably predict the long-term time dependent shaft resistance after the complete dissipation of pore water pressure.

The proposed approach confirms the bearing capacity evolution of used driven piles. The results of the theoretical approach and tests show consistent conclusions. The shaft resistance increases by 30%-50% due to the aging effect. This means that used piles can meet new building's demand of bearing capacity. The proposed method reveals the potential of recycling of used piles in situ. The proposed method can not only provide a reliable way to evaluate the bearing capacity development of used piles, but can be used to guide pile foundation design of future new buildings.

6. Factor analysis

Eqs. (11) and (12) show that the viscoplastic component of the volumetric strain is a variable that depends on the secondary compression index α and coefficient of (negative) dilatancy D. Therefore, it is reasonable to analyze the effects of α and D. In this section, results for unit shaft resistance with different α and D are presented.

Three different α values (0.0023, 0.0033, and 0.0043) and three D values (0.06, 0.07, and 0.08) are applied to analyze their influence. These different values change of the basis of the example at a depth of 8.84 m of TP-3.

The computational results of f_s corresponding to different α values are illustrated in Fig. 8. It can be concluded from Fig. 8 that the unit shaft resistance has a larger growth rate with a smaller α values in the early stage. The unit shaft resistance corresponding to different α values is basically consistent over time. Fig. 9 shows the void ratio change and *QuOCR* with different α values. Fig. 9 indicates that the downward trend of the change rate of e becomes steeper with a lower α in the early stage, which results in an increased variation rate of *QuOCR* with α in the stage. This phenomenon can be explained as the restrictions of $\upsilon(t)$ on $\dot{\upsilon}(t)$, which was well expressed in Eq. (9) and Fig. 4.

The computational results of f_s corresponding to each D value are shown in Fig. 10. Fig. 10(a) illustrates that the value of D has slight effect on the sides shear setup when the working load is zero. This is mainly because D reflects the effect of dilatancy and there is no shear stress in the surrounding soil when working load is zero. To study the effect of D, a 500 kN working load is assumed to act on the top of the pile. Fig. 10(b) indicates that a larger D value reduces the growth of unit shaft resistance and this trend becomes more obvious as time passing. The variations of the void ratio and quasi-overconsolidation ratio with the different D value are summarized in Fig. 11. The increase in D results in a slighter void ratio decrease. Acting in response, the increase in *QuOCR* is also limited. Eq. (14) and Eq. (15) presented in this paper can well interpret the impact of D on the void ratio change and *QuOCR*. Eq. (11) indicated that the shear-induced volumetric strain (dilatancy) is affected by D value, and dilatancy is increased with the growth of D, which imposes restrictions on the development of volume strain.

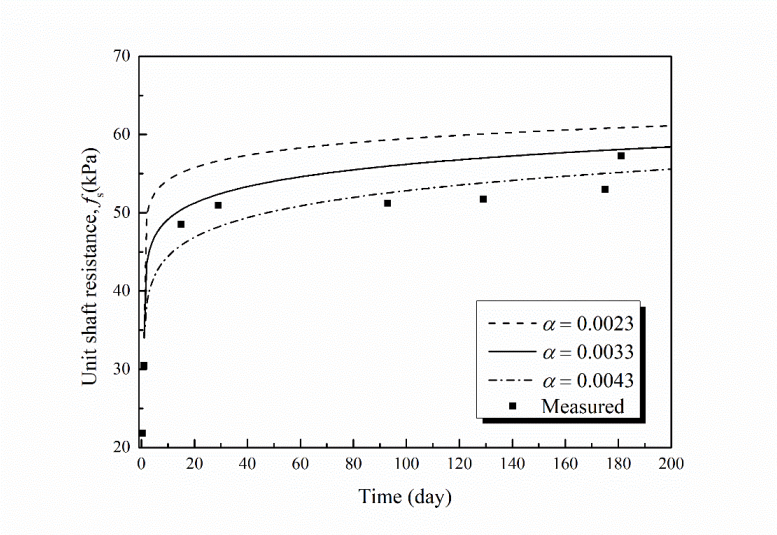

Fig. 8 Variation of unit shaft resistance with different values of α

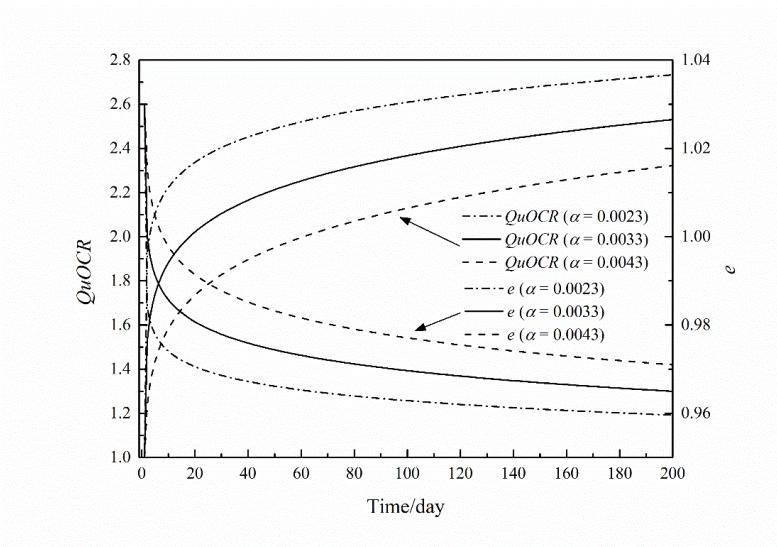

Fig. 9 Variation of QuOCR and e with different values of α

7. Conclusions

This study presents an analytic approach to determine the sides shear setup of reused driven piles in clay. The elasto-viscoplastic constitutive model and quasi-overconsolidation theory are employed to describe the ageing mechanism and strength change of the surrounding soil. The measured data of the test piles in Louisiana and the semi-logarithmic time function are cited to illustrate the effectiveness of the proposed method. This method confirms the potential value of the used pile and provides support for the design theory of piles reusing. Some influence factors of the sides shear setup are also analyzed according to the present method. The following conclusions can be drawn:

1. The proposed analytic approach can predict the long-term sides shear setup in clay. Comparisons between the predictions, the test pile program results and the semi-logarithmic time function show satisfactory agreement which indicate that the results calculated by the proposed approach are reasonable. Both the presented method and experimental data show the shaft resistance of the test piles has been increased by 30%-50% due to the ageing effect.
2. The gain of soil strength is the main reason of the long-term side shear setup of a driven pile in clay, which shows that the used pile can be reused for the foundation of a new building. The volumetric strain is properly determined by the nonstationary flow surface (NSFS) theory that reflects the restriction on the volumetric strain rate.
3. The secondary compression index and coefficient of dilatancy have a pronounced effect on the long-term side shear setup. The unit shaft resistance grows faster with a lower secondary compression index in the early stage. A higher value of D limits the growth of the unit shaft resistance and the restrictive effect becomes more obvious with time.

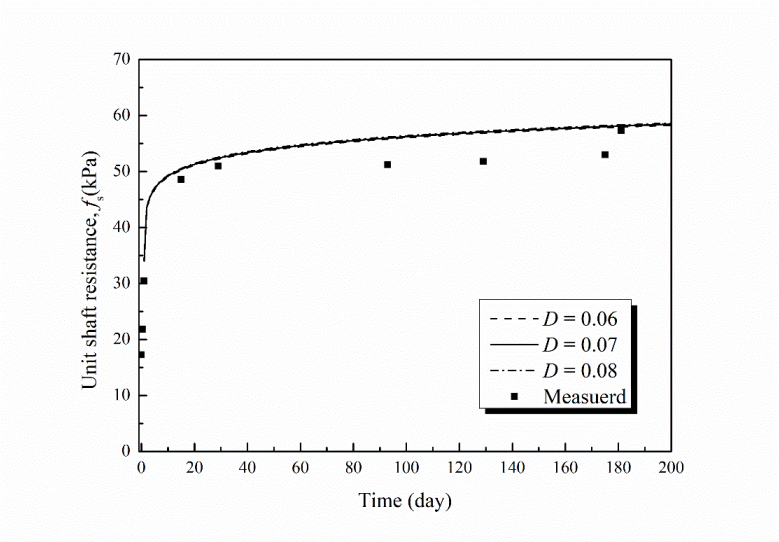

(a) P=0

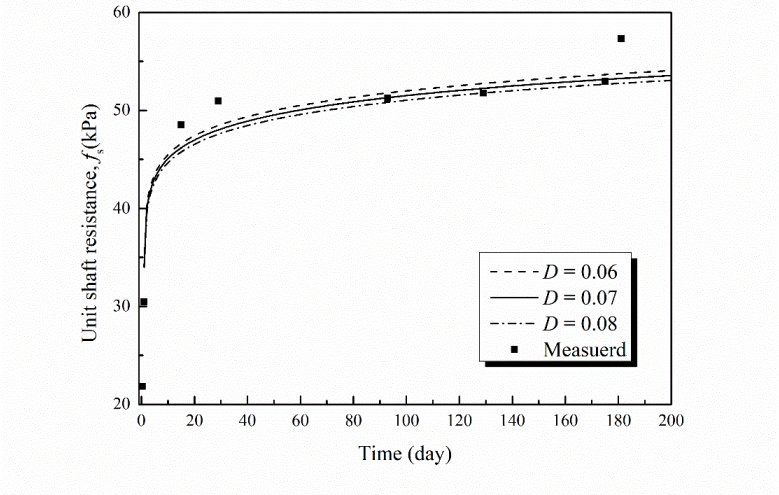

(b) P=500kN

Fig. 10 Variation of unit shaft resistance with different values of D

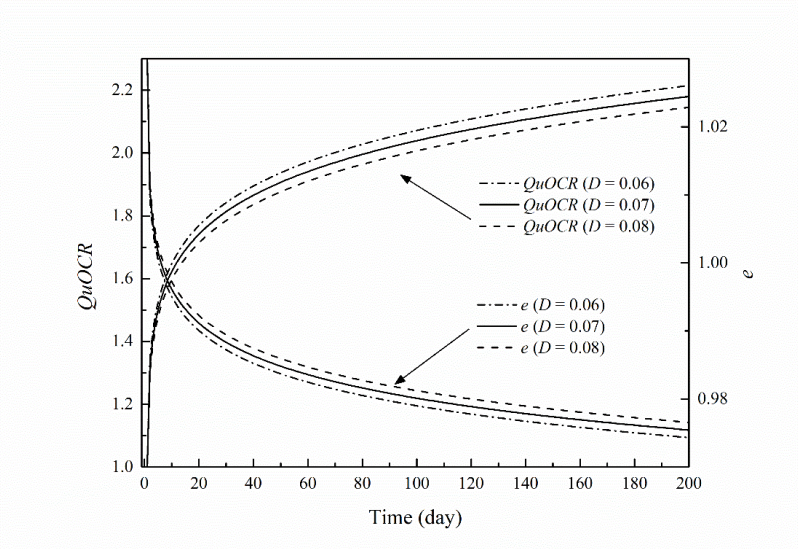

Fig. 11 Variation of *QuOCR* and *e* with different values of D (P=500kN)

Acknowledgments

The research work presented here was supported by the National Natural Science Foundation of China (Grant 52108328) and Soft Science Project of Shanghai Science and Technology Innovation Plan (Grant 22692193700). The financial supports are greatly appreciated.

References

Abu-Farsakh, M., Haque, Md. N. and Chen, Q. (2016), "Field instrumentation and testing to study set-up phenomenon of piles driven into Louisiana clayey soils", *Final Report of LTRC Project*, Report No. FHWA/LA.15/562.

Augustensen, A.H., Andersen. L.V. and Sørensen, C.S. (2005), "Time function for driven piles in clay", *Available from the Department of Civil Engineering*, Aalborg University, Denmark, Internal report, ISSN: 1398-6465 R0501.

Augustesen, A.H., Liingaard, M. and Lade, P.V. (2004), "Evaluation of time-dependent behavior of soils", *Int. J. Geomech.*, **4**(3), 137-156. https://doi.org/10.1061/(ASCE)1532-3641(2004)4:3(137).

Axelsson, G. (1998), "Long-term increase in shaft capacity of driven piles in sand", *Proceedings of the 4th International Conference on Case Histories in Geotechnical Engineering*, St. Louis, Missouri, March: 301-308. https://doi.org/10.1103/PhysRevLett.60.1201.

Axelsson, G. (2002), "A conceptual model of pile set-up for driven piles in non-cohesive soil", *Proceedings of the International Deep Foundations Congress*, Orlando, Florida, February. https://doi.org/10.1061/40601(256)6.

Basu, P., Prezzi, M., Salgado, R. and Chakraborty, T. (2014), "Shaft resistance and setup factors for piles jacked in clay", *J. Geotech. Geoenviron.*, **140**(3), 293-320. https://doi.org/0.1061/(ASCE)GT.1943-5606.0001018.

Borja, R.I. and Kavazanjian, E. (1985), "A constitutive model for the stress-strain-time behaviour of 'wet' clays", *Géotechnique*, **35**(3), 283-298. https://doi.org/10.1680/geot.1985.35.3.283.

Bowman, E.T. and Soga, K. (2003), "Creep, ageing and microstructural change in dense granular materials", *Soils Found.*, **43**(4), 107-117. https://doi.org/10.3208/sandf.43.4_107.

Bullock, P.J., Schmertmann, J.H., McVay, M.C. and Townsend, F. C. (2005a), "Side shear setup. I: Test piles driven in Florida", *J. Geotech. Geoenviron.*, **131**(3), 292-300. https://doi.org/10.1061/(asce)1090-0241(2005)131:3(292).

Bullock, P.J., Schmertmann, J.H., McVay, M.C. and Townsend, F. C. (2005b), "Side shear setup. II: results from Florida test piles", *J. Geotech. Geoenviron.*, **131**(3), 301-310. https://doi.org/10.1061/(ASCE)1090-0241(2005)131:3(301).

Chen, H.H., Li, L., Li, J.P. and Sun, D.A. (2021a), "A rigorous elastoplastic load-transfer model for axially loaded pile installed in saturated modified Cam-clay soils", *Acta Geotechnica*, **17**(2), 635-651. https://doi.org/10.1007/s11440-021-01248-z.

Chen, H.H., Li, L., Li, J.P. and Sun, D.A. (2021b), "A generic analytical elastic solution for excavation responses of an arbitrarily-shaped deep opening under biaxial in-situ stresses", *Int. J. Geomech.*, **22**(4), 0402202. https://doi.org/10.1061/(ASCE)GM.1943-5622.0002335.

Chen, H. H. and Mo, P. Q. (2022), "An undrained expansion solution of cylindrical cavity in SANICLAY for K0-consolidated clays", *J Rock Mech Geotech*. https://doi.org/10.1016/j.jrmge.2021.10.016

Chen, H.H. and Zhang, L.Y. (2022), "A machine learning-based method for predicting end-bearing capacity of rock-socketed shafts", *Rock Mech. Rock Eng*., https://doi.org/10.1007/s00603-021-02757-9.

Chong, S.H., Shin, H.S. and Cho, G.C. (2019), "Numerical analysis of offshore monopile during repetitive lateral loading", *Geomech. Eng.*, **19**(1), 79-91. https://doi.org/10.12989/gae.2019.19.1.079 .

Chou, J. and Yeh, K. (2015), "Life cycle carbon dioxide emissions simulation and environmental cost analysis for building construction", *J. Clean. Prod.*, **101**, 137-147. https://doi.org/10.1016/j.jclepro.2015.04.001.

Cui, J.F., Li, J.P. and Zhao, G.W. (2019), "Long-term time-dependent load-settlement characteristics of a driven pile in clay", *Comput. Geotech.*, **112**, 41-50. https://doi.org/10.1016/j.compgeo.2019.04.007.

Cui, J.F., Rao, P.P., Li, J.P., Chen, Q.S. and Nimbalkar, S. (2022), "Time-dependent evolution in bearing capacity of driven piles in clays combining installation, consolidation and subsequent loading", *Proceedings of the Institution of Civil Engineers - Geotechnical Engineering*, England, February, 1-47. https://doi.org/10.1680/jgeen.21.00200.

Doherty, P. and Gavin, K. (2013), "Pile aging in cohesive soils", *J. Geotech. Geoenviron.*, **139**(9), 1620-1624. https://doi.org/10.1061/(ASCE)GT.1943-5606.0000884.

Huang, S.M. (1988), "Application of dynamic measurement on long H pile driven into soft ground in Shanghai", *Proceedings of the 3rd Conference on Application of Stress-Wave Theory to Pile*, Ottawa, Canada.

Karim, M.R. and Gnanendran, C.T. (2014), "Review of constitutive models for describing the time dependent behaviour of soft clays", *Geomech. Geoengin.*, **9**(1), 36-51. https://doi.org/10.1080/17486025.2013.804212.

Ko, J., Cho, J. and Jeong, S. (2018), "Analysis of load sharing characteristics for a piled raft foundation", *Geomech. Eng.*, **16**(4), 449-461. https://doi.org/10.12989/gae.2018.16.4.449.

Kou, H.L., Chu, J., Guo, W. and Zhang, M.Y. (2017), "Pile load test of jacked open-ended prestressed high-strength concrete pipe pile in clay", *Proceedings of the Institution of Civil Engineers-Geotechnical Engineering*, **171**(3), 243-251. https://doi.org/10.1680/jgeen.16.00083.

Kou, H.L., Chu, J., Guo, W. and Zhang, M.Y. (2016), "Field study of residual forces developed in pre-stressed high-strength concrete (PHC) pipe piles", *Can Geotech. J.*, **53**(4), 696-707. https://doi.org/10.1139/cgj-2015-0177.

Kou, H.L., Guo, W. and Zhang, M.Y. (2016), "Field study of set-up effect in open-ended PHC pipe piles", *Mar. Georesour. Geotec.*, **38**(8), 939-946. https://doi.org/10.1080/1064119X.2015.1133742.

Li, L., Chen, H.H., Li, J.P. and Sun, D.A. (2021), "An elastoplastic solution to undrained expansion of a cylindrical cavity in SANICLAY under plane stress condition", *Comput. Geotech.*, **132**, 103990. https://doi.org/10.1016/j.compgeo.2020.103990.

Li, L., Li, J.P. and Sun, D.A. (2016), "Anisotropically elasto-plastic solution to undrained cylindrical cavity expansion in K0-consolidated clay", *Comput. Geotech.*, **73**, 83-90. https://doi.org/10.1016/j.compgeo.2015.11.022.

Li, L., Li, J.P., Sun, D.A. and Gong, W.B. (2017a), "Analysis of time-dependent bearing capacity of a driven pile in clayey soils by total stress method", *Int. J. Geomech.*, **17**(7), 04016156. https://doi.org/10.1061/(ASCE)GM.1943-5622.0000860.

Li, L., Li. J.P., Sun, D.A. and Zhang, L.X. (2017b), "Time-dependent bearing capacity of a jacked pile: An analytical approach based on effective stress method", *Ocean Eng.*, **143**, 177-185. https://doi.org/10.1016/j.oceaneng.2017.08.010.

Liingaard, M., Augustesen, A. and Lade, P.V. (2004), "Characterization of models for time-dependent behavior of soils", *Int. J. Geomech.*, **4**(3), 157-177, https://doi.org/10.1061/(ASCE)1532-3641(2004)4:3(157).

Li, Y.N. and Changm, L. (2022), "A log-spiral limit equilibrium analysis for passive earth pressure under the effect of unsaturated seepage conditions", *Eur. J. Environ. Civ. Eng.*, 1-19. https://doi.org/10.1080/19648189.2022.2043942.

Matsuoka, H, Yao, Y.P., and Sun, D.A. (1999), "The cam-clay models revised by the SMP criterion", *Soils Found.*, **39**(1), 81-95. https://doi.org/10.3208/sandf.39.81.

Mesri, G. and Godlewski, P.M. (1977), "Time and stress-compressibility interrelationship", *J. Geotech. Eng. Div.*, **103**(5), 417-430, https://doi.org/10.1016/0148-9062(77)91005-1.

Mo, P.Q. and Yu, H.S. (2017), "Undrained cavity expansion analysis in a unified state parameter model for clay and sand", *Géotechnique*, **67**(6), 503-515. https://doi.org/10.1680/jgeot.15.P.261.

Mo, P.Q. and Yu, H.S. (2018), "Drained cavity expansion analysis with a unified state parameter model for clay and sand", *Can Geotech. J.*, **55**(7), 1029-1040. https://doi.org/10.1139/cgj-2016-0695.

Perzyna, P. (1963), "The constitutive equations for work-hardening and rate sensitive plastic materials", *Proceeding of Vibration Problems*, Warsaw, **4**(4), 281-290.

Perzyna, P. (1966), "Fundamental problems in viscoplasticity", *Adv. Appl. Mech.*, **9**(3), 244-377, https://doi.org/10.1016/S0065-2156(08)70009-7.

Potts, D.M. and Martins, J.P. (1982), "The shaft resistance of axially loaded piles in clay", *Géotechnique*, **32**(4), 369-386. https://doi.org/10.1680/geot.1982.32.4.369.

Qiao, Y., Ferrari, A., Laloui, L. and Ding, W. (2016), "Nonstationary flow surface theory for modeling the viscoplastic behaviors of soils", *Comput. Geotech.*, **76**, 105-119. https://doi.org/10.1016/j.compgeo.2016.02.015.

Randolph, M.F. and Wroth, C.P. (1981), "Application of the failure state in undrained simple shear to the shaft capacity of driven piles", *Géotechnique*, **31**(1), 143-157. https://doi.org/10.1680/geot.1981.31.1.143.

Satake, M. (1989), "Mechanics of granular materials", *J. Geogr.*, **98**(6), 798-805. https://doi.org/10.5026/jgeography.98.6_798.

Sekiguchi, H. (1977a), "Rheological characteristics of clays", *Proceedings of the 9th International Conference on Soil Mechanics and Foundation Engineering*, Tokyo, Japan, January.

Sekiguchi, H. (1977b), "Induced anisotropy and time dependency in clays", *Proceedings of the 9th International Conference on Soil Mechanics and Foundation Engineering*, Tokyo, Japan, January.

Sekiguchi, H. (1984), "Theory of undrained creep rupture of normally consolidated clay based on elasto-viscoplasticity", *Soils Found.*, **24**(1), 129-147. https://doi.org/10.3208/sandf1972.24.129.

Sekiguchi, H. (1985), "Macrometric approaches-static-intrinsically time dependent constitutive laws of soils", *Proceedings of the Discussion Session, 11th International Conference on Soil Mechanics and Foundation Engineering*, San Francisco, U.S.A.

Shibata, T. (1963), "On the volume changes of normally-consolidated clays", *Disaster prevention Research Institute*, Kyoto University, **6**, 128-134. https://doi.org/10.2472/jsms.12.264.

Sivasithamparam, N., Karstunen, M. and Bonnier, P. (2015), "Modelling creep behaviour of anisotropic soft soils", *Comput. Geotech.*, **69**, 46-57. https://doi.org/10.1016/j.compgeo.2015.04.015.

Skov, R. and Denver, H. (1988), "Time dependence of bearing capacity of pile", *Proceedings of the 3rd Conference on Application of Stress-Wave Theory to Pile*, Ottawa, Canada.

Terzaghi, K. and Peck, R.B. (1968), *Soil mechanics in engineering practice: 2nd Ed.*, New York, U.S.A.

Thompson, W.R., Lloyd, H. and Steven, S. (2009), "Test pile program to determine axial capacity and pile setup for the Biloxi bay bridge", *DFI Journal-The Journal of the Deep Foundations Institute*, **3**(1), 13-22. https://doi.org/10.1179/dfi.2009.002.

Wijayasundara, M., Mendis, P. and Crawford, R.H. (2018), "Integrated assessment of the use of recycled concrete aggregate replacing natural aggregate in structural concrete", *J. Clean Prod.*, **174**, 591-604. https://doi.org/10.1016/j.jclepro.2017.10.301.

Xiao, J., Zhang, K. and Akbarnezhad, A. (2018a), "Variability of stress-strain relationship for recycled aggregate concrete under uniaxial compression loading", *J. Clean Prod.*, **181**, 753-771. https://doi.org/10.1016/j.jclepro.2018.01.247.

Xiao, J., Wang, C., Ding, T. and Akbarnezhad, A. (2018b), "A recycled aggregate concrete high-rise building: structural performance and embodied carbon footprint", *J. Clean Prod.*, **199**, 868-881. https://doi.org/10.1016/j.jclepro.2018.07.210.

Xu, C.J., Ding, H.B., Luo. W.J., Tong, L.H. and Chen, Q.S. (2020), "Experimental and numerical study on performance of long-short combined retaining piles", *Geomech. Eng.*, **20**(3), 255-265. https://doi.org/10.12989/gae.2020.20.3.255.

Yang, C.Y., Li, J.P., Li, L. and Sun, D.A. (2021), "Expansion responses of a cylindrical cavity in overconsolidated unsaturated soils: A semi-analytical elastoplastic solution", *Comput. Geotech.*, **130**, 103922. https://doi.org/10.1016/j.compgeo.2020.103922.

Yang, L. and Liang, R. (2006), "Incorporating set-up into reliability-based design of driven piles in clay", *Can. Geotech. J.*, **43**(9), 946-955. https://doi.org/10.1139/t06-054.

Yin, Z.Y., Karstunen, M. and Hicher, P.Y. (2010), "Evaluation of the influence of elasto-viscoplastic scaling functions on modelling time-dependent behaviour of natural clays", *Soils Found.*, **50**(2), 203-214. https://doi.org/10.1002/nag.684.

Zhang, X.F., Ni, Y.S., Song, C.X. and Xu, D. (2020), "Study on large tonnage pile foundation load test system and field test of long rock-socketed pile", *Geomech. Eng.*, **21**(6), 565-570. https://doi.org/10.12989/gae.2020.21.6.565.

Zhou, C., Yin, J.H., Zhu, J.G. and Cheng, C.M. (2005), "Elastic anisotropic viscoplastic modeling of the strain-rate dependent stress-strain behaviour of K0-consolidated natural marine clays in triaxial shear tests", *Int. J. Geomech.*, **5**(3), 218-232. https://doi.org/10.1061/(ASCE)1532-3641(2005)5:3(218).

Zhou, H., Liu, H. L., Yin, F. and Chu, J. (2018), "Upper and lower bound solutions for pressure-controlled cylindrical and spherical cavity expansion in semi-infinite soil", *Comp. Geotech.*, **103**, 93-102. https://doi.org/10.1016/j.compgeo.2018.07.011.

Zou, J.F., Yang, T. and Deng, D.P. (2019), "Field test of the long-term settlement for the post-grouted pile in the deep-thick soft soil", *Geomech. Eng.*, **19**(2), 115-126. https://doi.org/10.12989/gae.2019.19.2.115.

GC

List of Notations

σ'_{zf}, σ'_{rf}, $\sigma'_{\theta f}$	Effective stresses components	$\dot{\upsilon}_0$	Rate of initial volumetric strain
σ'_{v0}, σ'_{h0}	In situ stress of surrounding soil	α	Secondary compression index
K_0	Earth pressure coefficient at rest	$\upsilon(t)$	Volumetric strain
p'_f	Mean stress at the critical region	t	Elapsed time
q_f	Deviator stress at the critical region	D	Coefficient of dilatancy
β	Parameter to simplify the expressions	$\bar{h}$	Parameter to simplify the expressions
p'_0	In-situ initial mean stress	$\bar{p}'$	Mean effective stress
η_p^*	Relative stress ratio	$\bar{q}$	Generalized stress deviator
OCR	Over consolidation ratio	C_a	Secondary consolidation coefficient
Λ	Plastic volumetric strain ratio	ω_L	Liquid limit
M	Stress ratio at critical state	t_c	Reference time
λ	Compression index	e_0	Initial void ratio
κ	Swelling (or recompression) index	υ^e	Elastic component
σ'_{t0}	Final effective stress	υ^{p}	Viscoplastic component
u_{e0}	Excess pore pressure	Δe	Variation of the void ratio
ξ	Effective stress transfer parameter	$QuOCR$	Quasi-over-consolidation ratio
ν'	Effective Poisson's ratio	s_u	Undrained shear strength
M^*	Relative stress ratio at critical state	f_s	Ultimate side shear
η_0	Initial stress ratio	τ_{zx}	Failure shear stress acting on the top of the sample of simple shear test
r_{p}	Plastic region radius	s_{p}	Shear strength of simple shear test
P	Axial load acting on pile	ϕ'	Effective internal friction angle
r_d	Pile radius	φ_f , ψ_f	Conversion parameter
l_1, l_2	Length of the triangular and rectangle distribution of shaft resistance	Q_0	Capacity when pore water pressure has dissipated
f_{0m}	Maximum shaft resistance along the pile	Δ_{10}	Empirical coefficient
f_0	Shaft resistance along the pile	f_{s0}	Side resistance when pore water pressure has dissipated
$\dot{\upsilon}(t)$	Rate of volumetric strain	Δ'_{10}	Side (segment) shear setup factor